

# SURFACE CHARACTERIZATION OF MID-T HEAT TREATED Nb SAMPLES TO INVESTIGATE THE ORIGIN OF RESIDUAL RESISTANCE

R. Ghanbari <sup>†</sup>, M. Wenskat, G. Kacha Deyu, W. Hillert,

Institute of Experimental Physics, University of Hamburg, Hamburg, Germany

L. Steder, D. Reschke, H. Weise, Deutsches Elektronen-Synchrotron DESY, Germany

## Abstract

Heat treatment of niobium (Nb) cavities in UHV is crucial for the RF performance in the later cryogenic tests and operation. Recently, a so-called “mid-T heat treatment” has exhibited very high quality factors for Nb cavities. In this way, the first set of mid-T heat treated samples were produced with cavities at Zanon Research & Innovation Srl and were tested and studied at DESY. The cavity performances improved as predicted, especially the BCS resistance. However, the residual resistance showed higher values than expected. Thus, the characterization of these samples is discussed, and the source of high residual resistance has been studied here in detail. We present our investigation on potential origins. For this, we used XPS and MOKE measurements to study the surface magnetic domains and related structures.

## INTRODUCTION

For over two decades, superconducting radio frequency (SRF) systems have been a key technology for modern accelerators, and their importance continues to grow. Comprehensive research and development efforts have led to optimized recipes for constructing and treating SRF Nb cavities, resulting in reliable performance and impressive accelerating fields of up to 30 MV/m in large-scale accelerator facilities like the European XFEL or LCLS-II [1,2]. Recently, a ground-breaking recipe was discovered: The “mid-T heat treatment”. The standard mid-T heat treatment is defined as heating for 3 hours at 300°C [3] and usually is applied on cavities which underwent coarse chemistry, outgassing and fine EP, so called “baseline treatment” [4]. Mid-T heating process is performed using commercial ultra high vacuum (UHV) furnaces followed by cleaning and assembly steps under air. Mid-T heat treatment yields a significant reduction in the absolute value of losses and an inversion of the dependency of losses on the applied accelerating field ( $E_{acc}$ ), which shows a rise of quality factor ( $Q_0$ ) culminating at an  $E_{acc}$  of about 16 MV/m, which is often referred to as an “anti-Q slope” ( $dQ_0/dE_{acc}>0$  or  $dR_s/dE_{acc}<0$ ) [5-8]. In-situ medium temperature heat treatment studies have shown very high-quality factors [5]. This modified process could potentially be applied to future accelerator cavities and has been rapidly reproduced by many groups, including our own [1, 9-14].

Our working hypothesis is that the interstitial oxygen reorganization is responsible for the reduction of losses by

tailoring the density of states in the most favorable way. The mid-T heat treatment also results in a significant reduction

of residual resistance ( $R_{res}$ ) when performed in-situ [5], which strongly suggests an involvement of the native oxide layer. Our group has already conducted extensive studies on the native oxide layer and found the existence of magnetic domains caused by oxygen vacancies, which create “dangling bonds” and act as magnetic impurities [15-17]. These dangling bonds have been proposed as a source of losses based on the Shiba theory [18, 19]. By using magneto-optic Kerr effect (MOKE) measurement, it is possible to probe these magnetic domains and compare various treatments. Additionally, X-ray photoelectron spectroscopy (XPS) measurement have shown evidence of the re-organization and formation of oxide layers [20, 21]. Combining these two methods holds great potential in shedding light on the origin of  $R_{res}$  and advancing our understanding.

## SURFACE RESISTANCE OF HEAT-TREATED CAVITIES

In 2021, due to the commissioning of the furnace infrastructure at DESY, a collaboration was established with Zanon to investigate the impact of mid-T heat treatments on SRF cavities. Following the heat treatment at Zanon, vertical performance tests at DESY were executed. Two sets of two 1.3 GHz single-cell baseline treated cavities were heated for 3 hours at 300 °C as a mid-T heat treatment. One set of cavities were heated completely open in one furnace run, while the other set had the flanges loosely covered by Nb foils to prevent potential cavity contamination by the furnace [22]. One baseline treated cavity per set was additionally heated for 48 hours at 120°C (the European XFEL recipe) as a “low-T heat treatment” [23] prior to the mid-T heat treatment. Further details regarding the treatments and the vertical RF tests be found in Ref. [6].

Figure 1 presents the results of surface resistance ( $R_s$ ), further classified into BCS resistance ( $R_{BCS}$ ) and  $R_{res}$  for mid-T heat treated cavities. All cavities show  $R_{BCS}$  values below 6nΩ and exhibit anti-Q slope behavior, consistent with previous studies at FNAL, IHEP and KEK [5, 10, 24]. The observed  $R_{res}$  values, ranging from 3 to 12 nΩ, are relatively high compared to the previously reported acceptable value [5]. The high  $R_{res}$  values for the mid-T heat treated cavities in Fig. 1 mask a clear reduction of  $R_s$ . The cavity 1AC2 which is treated without cap, exhibited the highest  $R_{res}$  value. The Cavity 1DE9 in Fig. 1(b) showed the best result in terms of  $R_{res}$ . This cavity underwent no

\* Work supported by Institute of Experimental Physics, University of Hamburg and Deutsches Elektronen-Synchrotron DESY

<sup>†</sup> rezvan.ghanbari@desy.de

low-T heat treatment before and was closed by caps during treatment. According to the variety of  $R_{\text{res}}$  ranges for these

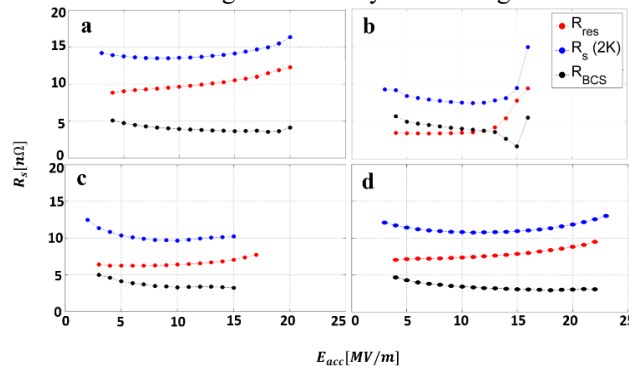


Figure 1: Surface resistance  $R_s$  (blue), calculated residual resistance  $R_{\text{res}}$  (red) and BCS resistance  $R_{\text{BCS}}$  (black) of the four different heat treated cavities: (a) 1AC2 heated at 300 °C for 3 hours without a cap, (b) 1DE9 heated at 300 °C for 3 hours with a cap, (c) 1DE7 heated first at 120 °C for 48 hours, then at 300 °C for 3 hours without a cap, and (d) 1DE5 heated first at 120 °C for 48 hours, then at 300 °C for 3 hours with a cap. See Ref. [6].

mid-T heat treated cavities, sample study is necessary to determine the origin of losses.

## SAMPLE STUDY AND OUR APPROACH

During the treatments, Nb baseline treated samples were also processed, with one sample heated alongside each mentioned cavity in the previous section. The samples were labelled as Niob 1 through Niob 4. Niob 1 was treated with 1AC2, which had the highest  $R_{\text{res}}$  value, was sent for MOKE measurement. Niob 2, Niob 4, and another sample called Niob 5 underwent XPS measurement and have also sent for MOKE measurements. Niob 2 and Niob 4 were treated with 1DE9 and 1DE5, respectively (See Fig. 1). Niob 5 is a low-T heat treated sample as a reference. The following section will present the results of the XPS measurements, MOKE measurement along with a comparison

of the remanence magnetization of Niob 1 with samples of other treatment studies. The result of MOKE measurements for Niob 2, 4, and 5 are being probed.

## RESULT

XPS measurements were performed on samples Niob 2, 4 and 5 which were under mid-T, low-T + mid-T and low-T heat treatments, respectively. The Nb 3d core peaks of XPS measurement are illustrated in Figure 2. For each sample, 6 curves with different second values of etching are plotted, and each higher second value represents deeper penetrated oxide layers on the surface. The Nb 3d region comprise a number of doublets with binding energies in descending order for Nb 3d at 207.6, 203.9, 202.6, and 202.0 eV, which are assigned to  $\text{Nb}_2\text{O}_5$ ,  $\text{NbO}$ ,  $\text{Nb}_x\text{O}$ , and metallic Nb components, respectively [20, 21]. The overlapping of the corresponding peaks of different oxides of niobium make the deconvolution of the Nb 3d line difficult. However, by comparing the 0 second etching curves of Fig. 2 (a), (b) and (c), it is found that in Fig. 2 (a) and (b), the major subpeak belong to  $\text{Nb}_2\text{O}_5$  peak, while in Fig. 2 (c), other subpeaks contribute to the curve, indicating less pentoxide for Niob 2 compared to Niob 4 and Niob 5. It is concluded that less pentoxide thickness is found on samples treated identically to cavities with lower residual resistance, and performing low-T heat treatment prior to mid-T heat treatment increase pentoxide layer thicknesses, mitigate the pentoxide reduction. Comparing the 60 seconds etching curves for these three samples show that the percentage of  $\text{NbO}$  and  $\text{Nb}_x\text{O}$  subpeaks are changed from Fig. 2 (a) to (c). The percentage of  $\text{NbO}$  decreased, whereas the  $\text{Nb}_x\text{O}$  peak increased. Surface magnetic order can be observed in oxides, and it is assumed that this is due to oxygen vacancies [15]. Hence, the magnetic order of samples Niob 1, Niob 2, Niob 4 and Niob 5 within the first 15 nm at room temperature were studied with using Kerr microscopy. Figure 3 shows an image taken with Kerr microscope

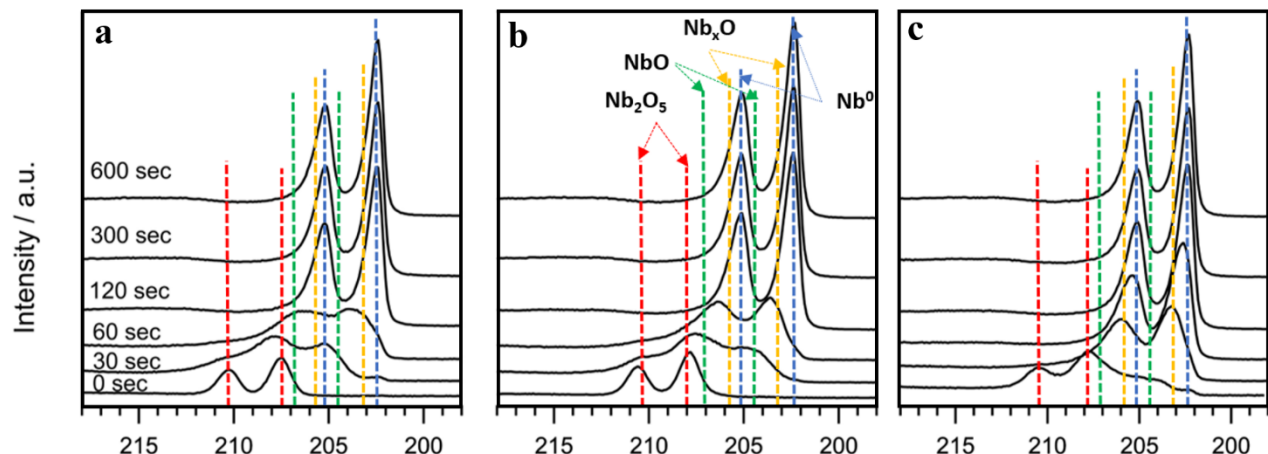


Figure 2: Etching profile of Nb 3d core peak using XPS measurement: (a) Niob 5, a reference sample heated for 48 hours at 120°C as a low-T heat treated sample, (b) Niob 2 treated first for 48 hours at 120°C, then for 3 hours at 300°C with the cavity 1DE09, (c) Niob 4 treated for 3 hours at 300°C with the cavity 1DE5. The dashed lines show the corresponding peaks for different oxide layers.

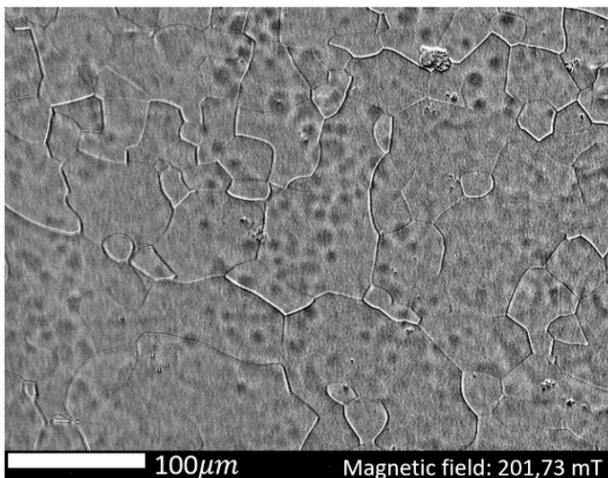


Figure 3: Kerr image of sample Niob 1 which was under mid-T heat treatment with cavity 1AC2 (see Fig. 1). Brighter areas are domains with a magnetization antiparallel to dark areas. The grain boundary structure is clearly visible as continuous lines. A spotted multidomain structure ( $d < 10 \mu\text{m}$ ), overlaying the grain boundaries and randomly distributed, is observed.

on Niob 1. The image displays a formation of a multidomain structure distributed across the sample surface. In Figure 4, the percentages of remanence magnetization for different treatments are presented. Niob 1 shows higher amount of residual magnetization compared to Niob 6 as another reference identical to Niob 5. This shows another correlation that a higher remanence magnetization is seen on the sample which is identically treated to that cavity 1AC2, which showed an increase in  $R_{\text{res}}$  after mid-T heat treatment. Therefore, a thicker pentoxide would contain more oxygen vacancies, which then could result in a higher remanent magnetization. This is further supported by the interesting result found for Niob 8, which was supposed to be another mid-T heat treated sample, but accidentally heated at higher vacuum pressure, knowingly leading to a further growth of pentoxide, and significantly a higher remanence magnetization is observed. In the contrary, the remanence magnetization of Niob 7&9 significantly decreased after the so-called N-infusion treatment [25, 26]. For this treatment, in general a reduction of the residual resistance of cavities compare to the regular European XFEL recipe is observed. Again, a correlation between this remanent magnetization and the residual resistance of corresponding cavities is found. Two assumptions have been put forward to explain this reduction. Firstly, it is possible that a thin N-monolayer was formed during the N-infusion, altering the substrate for pentoxide re-growth [25]. Alternatively, N-infusion may have reduced the hydrogen concentration near the surface, resulting in weaker coupled magnetic impurities reducing the remanence magnetization [26]. This further supports the hypothesis that the thickness of pentoxide layer and reorganization of NbO and Nb<sub>x</sub>O oxide layers, which can be controlled through heat treatments, affect the residual resistance of the cavity. Results of remanence magnetization for Niob 2, 4 and 5 are under analysis.

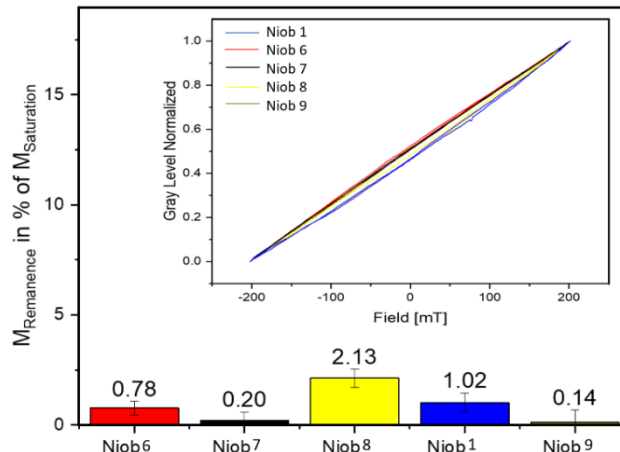


Figure 4: The percentage of remanence magnetization for different treatments: Niob 1 treated for 3 hours at 300°C with cavity 1AC2 (See Fig. 1), Niob 6 treated for 48h at 120°C as a reference sample, Niob 7&9 were under N-infusion treatment and Niob 8 heated for 3 hours at 300°C, accidentally at  $10^{-4}$  mbar. The inset illustrates different magnetization profile left behind on the surface of the samples after applying an external magnetic field.

and these results will provide valuable insights into correlations and help us better understand the origins.

## CONCLUSION

We started to explore the use of mid-T heat treatment as a promising path towards achieving cavities with higher quality factors while also achieving higher gradients. The treatments at Zanon had relatively large residual resistances that masked the reduction of  $R_s$ . The sample studies presented in this paper provide valuable insights into the impact of mid-T and low-T heat treatments on the surface properties of Nb samples. The XPS measurements indicate that the thickness of the Nb<sub>2</sub>O<sub>5</sub> layer is lower for samples treated identically to cavities with lower residual resistance, and performing a low-T heat treatment prior to mid-T heat treatment mitigates the pentoxide reduction. The MOKE measurements reveal variations in the remanence magnetization for different treatments and leads us to the conclusion that the niobium pentoxide contributes to the residual resistance, as it contains oxide vacancies acting as magnetic impurities. These magnetic impurities will then alter the density of states (DOS) in a detrimental way, according to the Shiba theory, and result in a higher surface resistance.

## ACKNOWLEDGEMENT

The authors would like to thank Zanon Research & Innovation Srl team, M. Aeschlimann (TUKL), C. Backes (TUKL) and M. Stahl (TUKL), N. Schäfer (TUDA), DESY cleanroom and RF-test operators. This work is partially funded by Helmholtz Association within the topic Accelerator Research and Development (ARD) of the Matter and Technologies (MT) Program and from the BMBF project 05H21GURB2.

## REFERENCES

[1] Reschke, D. *et al.*, “Performance in the vertical test of the 832 nine-cell 1.3 GHz cavities for the European X-ray Free Electron Laser”, *Phys. Rev. Accel. and Beams* vol. 20, no. 4, Apr. 2017, doi: 10.1103/PhysRevAccelBeams.20.042004

[2] Gonnella, D. *et al.*, “Industrialization of the nitrogen-doping preparation for SRF cavities for LCLS-II”, *Nucl. Instru. and Methods in Phys. Research Sec. A: Accel., Spect., Detect. and Assoc. Equip.* vol. 883, pp. 143–150, Mar. 2018, doi: 10.1016/j.nima.2017.11.047.

[3] Yang, Zhitao *et al.*, “Effective medium temperature baking of 1.3 GHz single cell SRF cavities”, *Physica C: Superconduct. and its Applic.* vol. 599, p. 1354092, Aug. 2022, doi: 10.1016/j.physc.2022.1354092.

[4] Aune, Bernard *et al.*, “Superconducting TESLA cavities”, *Phys. Rev. special topics-accel. and beams*, vol. 3, no. 9, Sep. 2000, doi: 10.1103/physrevstab.3.092001.

[5] S. Posen *et al.*, “Ultralow Surface Resistance via Vacuum Heat Treatment of Superconducting Radio-Frequency Cavities”, *Phys. Rev. Appl.*, vol. 13, no. 1, Jan. 2020, doi: 10.1103/physrevapplied.13.014024.

[6] L. Steder *et al.*, “Medium Temperature Treatments of Superconducting Radio Frequency Cavities at DESY”, in *Proc. LINAC’22*, Liverpool, UK, Aug.-Sep. 2022, pp. 840–843. doi: 10.18429/JACoW-LINAC2022-THPOGE22

[7] A. Grassellino *et al.*, “Nitrogen and argon doping of niobium for superconducting radio frequency cavities: a pathway to highly efficient accelerating structures”, *Superconductor Science and Technology*, vol. 26, no. 10, p. 102001, Aug. 2013, doi: 10.1088/0953-2048/26/10/102001.

[8] M. Martinello *et al.*, “Effect of interstitial impurities on the field dependent microwave surface resistance of niobium”, *Appl. Phys. Lett.*, vol. 109, no. 6, p. 062601, Aug. 2016, doi: 10.1063/1.4960801.

[9] F. He *et al.*, “Medium-temperature furnace baking of 1.3 GHz 9-cell superconducting cavities at IHEP”, *Supercond. Sci. Tech.*, vol. 34, no. 9, p. 095005, Aug. 2021, doi: 10.1088/1361-6668/ac1657.

[10] H. Ito, H. Araki, K. Takahashi, and K. Umemori, “Influence of furnace baking on Q-E behavior of superconducting accelerating cavities”, *Progr. of Theor. and Exp. Phys.* May 2021, doi: 10.1093/ptep/ptab056.

[11] M. Wenskat *et al.*, “Vacancy-Hydrogen Dynamics and Magnetic Impurities During Mid-T Bake”, in *Proc. SRF’21*, East Lansing, MI, USA, Jun.-Jul. 2021, pp. 342. doi: 10.18429/JACoW-SRF2021-TU0FDV03

[12] E. M. Lechner, J. W. Angle, F. A. Stevie, M. J. Kelley, C. E. Reece, and A. D. Palczewski, “RF surface resistance tuning of superconducting niobium via thermal diffusion of native oxide”, *Appl. Phys. Lett.*, vol. 119, no. 8, p. 082601, Aug. 2021, doi: 10.1063/5.0059464.

[13] M. Wenskat *et al.*, “Vacancy-Hydrogen Interaction in Niobium during Low-Temperature Baking”, *Sci. Rep.*, vol. 10, no. 1, May 2020, doi: 10.1038/s41598-020-65083-0.

[14] L. Steder and D. Reschke, “Statistical Analysis of the 120°C Bake Procedure of Superconducting Radio Frequency Cavities”, in *Proc. SRF’19*, Dresden, Germany, Jun.-Jul. 2019, pp. 444–447. doi: 10.18429/JACoW-SRF2019-TUP020

[15] M. Wenskat *et al.*, “Vacancy dynamics in niobium and its native oxides and their potential implications for quantum computing and superconducting accelerators”, *Phys. Rev. B* vol. 106, no. 9, Sep. 2022, doi: 10.1103/physrevb.106.094516

[16] T. F. Harrelson *et al.*, “Elucidating the local atomic and electronic structure of amorphous oxidized superconducting niobium films”, *Appl. Phys. Lett.*, vol. 119, no. 24, p. 244004, Dec. 2021, doi: 10.1063/5.0069549.

[17] E. Sheridan *et al.*, “Microscopic Theory of Magnetic Disorder-Induced Decoherence in Superconducting Nb Films”, doi: 10.48550/arXiv.2111.11684

[18] Proslier, M. Kharitonov, M. Pellin, J. Zasadzinski, and Ciovati, “Evidence of Surface Paramagnetism in Niobium and Consequences for the Superconducting Cavity Surface Impedance”, *IEEE Trans. Appl. Supercond.* vol. 21, no. 3, pp. 2619–2622, Jun. 2011, doi: 10.1109/tasc.2011.2107491.

[19] M. Kharitonov, T. Proslier, A. Glatz, and M. J. Pellin, “Surface impedance of superconductors with magnetic impurities”, *Phys. Rev. B.*, vol. 86, no. 2, Jul. 2012, doi: 10.1103/physrevb.86.024514.

[20] M. Delheusy, “X-ray investigation of Nb/O interfaces”, PhD thesis, Universität Stuttgart, Stuttgart, Germany, 2008.

[21] A. Dangwal Pandey *et al.*, “Surface characterization of nitrogen-doped Nb (100) large-grain superconducting RF cavity material”, *Jour. of Mater. Sci.*, vol. 53, no. 14, pp. 10411–10422, Apr. 2018, doi: 10.1007/s10853-018-2310-8.

[22] M. Wenskat *et al.*, “Nitrogen infusion R&D at DESY a case study on cavity cut-outs”, *Supercond. Sci. and Tech.*, vol. 33, no. 11, p. 115017, Oct. 2020, doi: 10.1088/1361-6668/abb58c.

[23] G. Ciovati, “Effect of low-temperature baking on the radio-frequency properties of niobium superconducting cavities for particle accelerators”, *Jour. of Appl. Phys.* vol. 96, no. 3, pp. 1591–1600, Aug. 2004, doi: 10.1063/1.1767295.

[24] Q. Zhou, F.-S. He, W. Pan, P. Sha, Z. Mi, and B. Liu, “Medium-temperature baking of 1.3 GHz superconducting radio frequency single-cell cavity”, *Radiat. Detect. Technol. Methods*, vol. 4, no. 4, pp. 507–512, Oct. 2020, doi: 10.1007/s41605-020-00208-7.

[25] K. Zhussupbekov *et al.*, “Oxidation of Nb(110): atomic structure of the NbO layer and its influence on further oxidation”, *Scientif. Repo.*, vol. 10, no. 1, Mar. 2020, doi: 10.1038/s41598-020-60508-2.

[26] P. Esquinazi, W. Hergert, D. Spemann, A. Setzer, and A. Ernst, “Defect-Induced Magnetism in Solids”, *IEEE Transactions on Magnetics*, vol. 49, no. 8, pp. 4668–4674, Aug. 2013, doi: 10.1109/tmag.2013.2255867.